# Fine Pitch Interconnection and Packaging Studies for Hybrid Electronics with Aerosol Jet Printed Particle-Free Ag Ink

Abdullah S. Obeidat[1,4], Dylan Richmond[3], Jordan Howard-Jennings[3,4], Ashraf Umar[2,4], Riadh Al-Haidari[1,4], Mohammed Alhendi[1], Behnam Garakani[3], Detlef-M. Smilgies[3,4], Mark D. Poliks[1,3,4]
[1]Dept. of Systems Science and Industrial Engineering, State University of New York at Binghamton, USA
[2]Dept. of Electrical and Computer Engineering, State University of New York at Binghamton, USA
[3]Materials Science and Engineering Program, State University of New York at Binghamton, USA.
[4]Center of Advanced Microelectronics Manufacturing (CAMM), State University of New York at Binghamton, USA

## Abstract

Additive manufacturing of conductive interconnects has become essential in the electronic industry due to the requirements of having smaller electronic components with high performance and producing functional electronics that meet the applications demand. Thus, fabricating conductive lines and patches is key to reduce the challenges of mechanical and thermal reliability associated with advanced electronic technologies. In this work, high-resolution conductive interconnects were fabricated by aerosol jet printing (AJP) across different substrates using a novel particle-free silver ink. The conductivity of the metallic ink was assessed after post-processing at various curing conditions and methods. The printing process parameters of the particle-free ink were optimized to yield high-quality printed features and to investigate the printed film's continuity on a non-flat surface, including printing from the top of a silicon die to a flexible substrate. The current carrying capacity of the printed particle-free silver ink on NEA 123 material was evaluated and compared against a commonly used nanoflake-based silver ink by performing a current sweep increasing the current by 5mA every 10 seconds until failure.

In this research, conductive interconnects with sub-micron thickness have been obtained. Photonic curing using PulseForge system was found to improve the conductivity at energy density of 3.22 J/cm$^2$ to four times the conductivity of a conventional convection oven curing. The enhancement in conductivity appears to be due to the changes in the film's microstructure, forming metallic connections between the needle-shaped crystallized grains as revealed by X-ray microtomography. The particle-free ink can be used for irregular surfaces with smooth transitions between the electronic components. Furthermore, the current carrying capacity tests show the printed interconnect's resistivity increased and then reduced during the test before failure; the failure of the particle-free ink occurred at 2.022 x $10^5 \pm 0.2$ A/cm$^2$ compared to 0.99 x $10^5 \pm 0.18$ A/cm$^2$ for the nanoflake-based silver ink which makes the particle-free ink an attractive material for high-power electronics applications. Our findings assist the application of flexible hybrid electronics and electronic packaging by providing significant guidelines for electronics manufacturers.

## Key words

*Aerosol Jet Printing, flexible hybrid electronics, fine pitch interconnects, current carrying capacity.*

## I. Introduction

Miniaturization is the main trend of electronic components which requires development in the materials and printing techniques [1]. Printed electronics fabrication techniques present multiple advantages in the electronics industry over their conventional counterparts, including less material waste, lower costs, compatibility with "Roll-to-roll" (R2R) manufacturing, and applicability to various types of substrates. Progress in printed electronics is subject to the development of materials, including ink and substrate properties, advanced printing techniques suitable for high-volume manufacturing and specific system design [2-4].

Flexible and hybrid electronics (FHE) enables advanced applications that cannot be obtained by conventional electronics. Combining flexible electronics and rigid electronic components yields highly functional and reliable devices [3]. Aerosol jet printing (AJP) is widely used to print fine and small features down to 10 µm, as it can be used with a wide range of materials and permits printing on 3D objects [3], [5]. Printing on irregular surfaces is crucial to enable the fabrication of devices with complex shapes and conformal devices that can be used in various applications such as wearable electronics and the Internet of Things (IoT) industry [6]. Post-processing treatment is required after printing to solidify the ink, enhance adhesion, and improve conductivity. Photonic annealing is an advanced curing method that uses a Xenon flash lamp to deliver high energy light pulses within the milli- to micro-second time regime. It is suitable for low glass transition temperature (Tg) substrates and thin films, and it is compatible with Roll-to-Roll (R2R) production [7].

Particle-free inks contain soluble metal-organic compounds and additives that help achieve stability, increased adhesion properties, and the desired conductivity. They are becoming increasingly attractive due to their flexibility in preparation, higher conductivity compared to conventional inks, longer storage stability due to avoidance of particle precipitation and aggregation over time, and reduced likelihood of nozzle clogging during the printing process. Particle-free inks are created from specifically chosen metal salts or complexes that dissolve in a liquid medium and can be changed to pure metal by thermal decomposition treatment. Several factors are to be considered when selecting the particle-free ink: (i) the metal content and conductivity, (ii) adhesion classification to the substrate, (iii) optimizing the printing process to achieve long printing stability and high-quality features [1], [8-10].

The current carrying capacity test for printed electronics evaluates the printed traces to carry increasing amounts of electrical current until failure. The test includes applying an electrical current that increases gradually at a defined step rate across the printed features and monitoring the conductivity changes against current density. Heat dissipation is generated from the printed traces as the electrical current flows; thus the trace temperature will increase and impact the adhesion between the trace and the substrate as well as damage the substrate and the trace due to the high thermal stresses. Several factors affect the current handling capacity in the printed traces including the material microstructure, the substrate's thermal properties and the trace's cross-section area [11-13].

In this work, the printing stability of the particle-free silver ink was investigated by optimizing the process parameters of the aerosol jet printer (AJP). The electrical conductivity of the particle-free ink was improved using photonic curing and compared with thermal curing. X-ray and SEM images were taken to study the microstructure changes of the printed traces. The ink continuity on irregular surfaces and between a Si die and a film of PET was investigated to understand the particle-free ink's capabilities and limitations. The current carrying capacity of the particle-free ink was evaluated to ensure reliable and high performance of printed electronic traces.

## II. Experimental Section

### *A. Printing Techniques*

An aerosol jet printer 3X system from Optomec, Inc. Albuquerque, USA was used to print interconnects on flexible polyethylene terephthalate (PET) substrates with 5 mils thickness. The thin films were printed using an particle-free Ag ink that has less than 5 cP viscosity which makes it suitable for the AJP ultrasonic atomizer system. In this atomization technique, the ink is placed in a glass container and vibrated via ultrasonic energy generated by a transducer. The shockwave in the liquid breaks the material in the container into small droplets that can be transported with a carrier gas, in our case nitrogen ($N_2$). The aerosol droplets will transfer to the deposition head. A sheath gas flow of $N_2$ is applied to the nozzle to control the ink stream deposition to the desired substrate and focus the aerosol flow. The printing process system was optimized to print thin features [14],[15],[16],[17]. For hybrid electronics a dispensing system (NORDSON EFD PRO4) from Nordson was used to dispense dielectric materials (NEA 123) to build a ramp around the Si die to enable a smooth transition between the Si die and the substrate.

### *B. Photonic Curing*

Curing thin films printed on PET substrate is a challenge due to PET's low glass transmission temperature (Tg). Therefore, photonic curing using the “PulseForge® Invent” tool from Novacentrix was used to cure the printed traces by applying high energy within a short time provided by Xenon flash lamp. Due to a short pulse length only small amounts of heat are transferred to the substrate material. The process parameters, including the voltage, number of pulses and envelope time were optimized to maximize the conductivity of the printed traces. A Keyence VK-X1050 laser 3D microscope was used to characterize the printed features, including the printing quality, topography and dimensions determination. Some samples were further characterized with SEM (Zeiss Supra) and X-ray microtomography (Zeiss X-Radia).

## III. RESULTS AND DISCUSSION

### *A. Particle-free Ink Printing Stability*

Exploring the stability of newly developed particle-free inks is essential in the electronic field, enabling more reliable and efficient devices. Several experiments were performed to optimize the printing process parameters of the particle-free ink. The current level that affects the amplitude of the vibration shall not be more than 300 mA to be able print for a long period. Fig.1 shows the cross-section area of printed films versus printing time. Three and five layers of ink were printed in the same experiment and the cross-section area of the printed samples remained almost the same during a 60 minute printing period. This demonstrates that ink stability is achievable with the AJP process, allowing for highly accurate and repeatable prints.

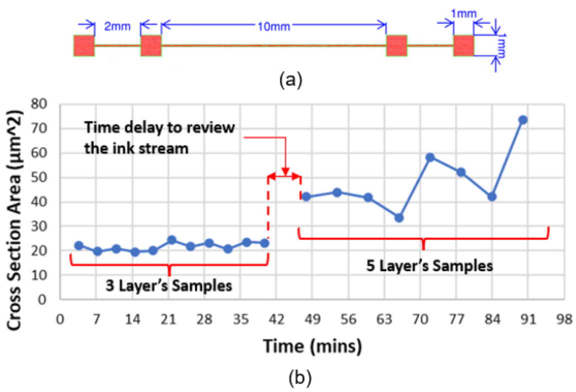


Fig. 1: (a) Printed film design, (b) Printed films cross-section area vs. printing time.

### *B. Particle-free Ag Ink Characterization*

Evaluating the adhesion of inks on flexible substrates is crucial for having a new generation of bendable and wearable electronics, ensuring the durability and reliability of devices in real-life applications. A cross-hatch adhesion test was performed based on the ASTM D3359 standard on various substrates, including PET, glass, PI and NEA123 printed on a glass substrate. The results show that the particle-free ink has excellent adhesion to PET and NEA 123 with a “5B” classification, while the adhesion was poor on PI and glass with “1B” and “0B” classification, respectively.

Given the current trend in the electronics industry to reduce the footprint and size of electronic components, work towards improving the efficiency and the performance of electronic devices is necessary. Therefore, to evaluate the functionality of the novel particle-free Ag ink, multiple 10 mm length traces were printed on glass substrates with multiple layers to evaluate the resolution that can be obtained with particle-free ink. Fig.2 shows the obtained thicknesses and widths of the traces with 1, 3, 5, 8 and 10 layers. It is observed that all printed traces are less than 1 µm even with 10 layers. The width of the tallest deposits remained below 40 µm. The ultra-thin layers of the particle-free ink enable the formation of precise electronic pathways, which is important for the miniaturization of electronic devices without affecting their performance.

### *C. Conductivity Improvement of Particle-free Ag Ink*

Improving the conductivity of printed traces creates highly powerful and efficient electronics. Enhancing the trace conductivity is necessary to minimize electronics while still improving their performance and capabilities. Two curing methods were used for the particle-free ink printed features; conventional oven and photonic annealing. Printed traces on

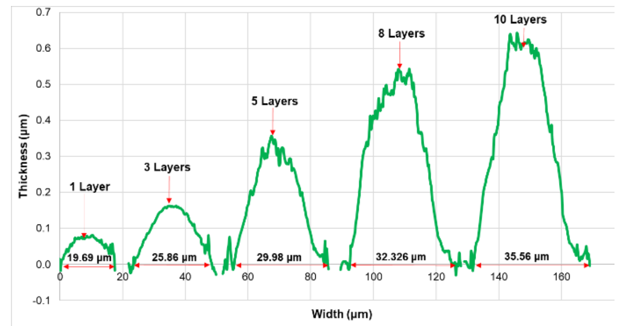


Fig. 2: Printed traces profile with several layers using silver particle-free ink.

glass substrates were cured in a Binder ED 56 convection oven at 150°C, 200°C and 250°C for one hour. The average conductivity of the cured sample at 150°C is 1.26x$10^6$ S/m, at 200°C is 14.2x$10^6$ S/m and at 250°C is 15.79x$10^6$ S/m. Curing at 250°C for 1 hour provided the highest conductivity; however, at these conditions, cracks are observed in the traces. Therefore, curing at 200°C provides the optimum conductivity reaching 22.6% of the bulk silver conductivity. As shown in Fig.3, the thermal curing in the oven at 250°C for 1 hour crystalized the dissolved silver to form physically contacted grains.

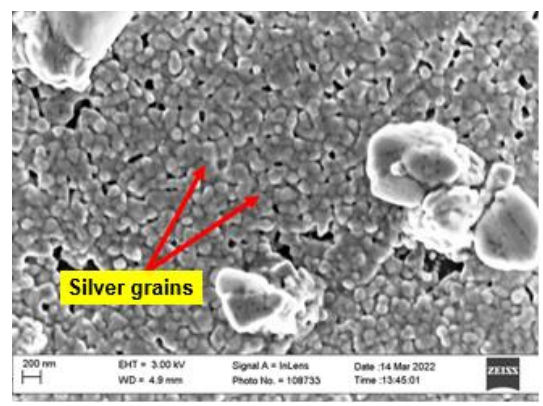


Fig. 3: SEM image of particle-free ink cured at 250°C for 1 hr. (50K magnification)

The PET substrate has dimensional stability up to 150°C, making it sensitive to degradation during curing [16]. Therefore, photonic curing was used as an alternative to anneal the printed features using the “PulseForge® Invent” tool from Novacentrix. Fig.4 shows the achieved conductivity of printed films at different photonic energy levels. The highest conductivity achieved was 42.14x$10^6$ S/m at 4.82 J/cm$^2$. However, cracks were noticed in the printed films at this energy and at 7.85 J/cm$^2$. Therefore, the optimum conductivity (39.23x$10^6$ S/m) is achieved without physical damage on the traces at 3.81 J/cm$^2$ under optimized parameters of 320 volts, 2 pulses and a 10 milliseconds envelope time for the Xenon flash lamp. After curing under the optimized photonic parameters, the film conductivity reached 62% of the bulk silver conductivity, which is excellent in the printed electronic field.

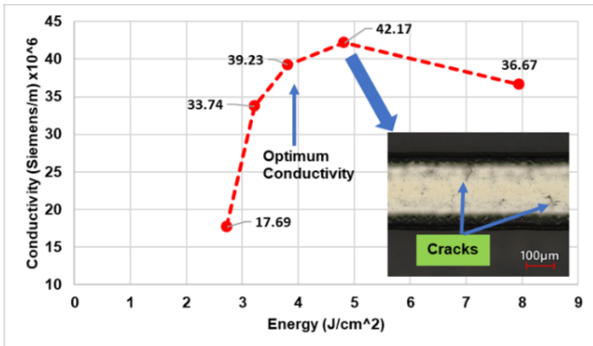


Fig. 4: Printed films conductivity at various photonic energy levels.

X-ray microtomography images were taken using Zeiss X-Radia to investigate the effect of the photonic curing on the microstructure of the printed films and compare it with a sample cured in the convection oven at 140°C for 1 hour. As shown in Fig.5 (a), small grains were formed after thermal annealing. Part (b) of the same figure highlights the morphology of aerosol jet-printed traces of particle-free silver ink after exposure to flash annealing. The dissolved silver salts formed a network of connected metallic needles improving the conductivity to four times the conductivity of a thermally annealed films.

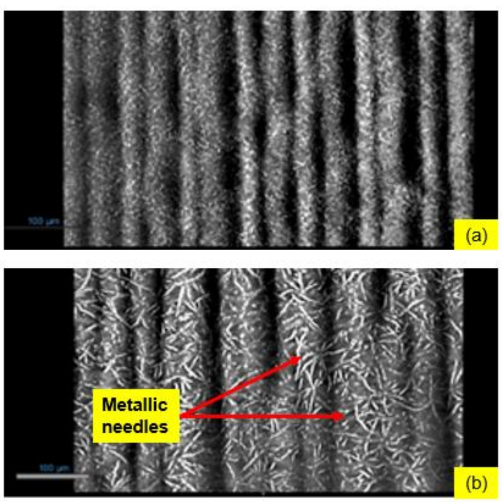


Fig. 5: X-ray microtomography images of printed particles free ink after (a) Thermal annealing, (b) Photonic/flash annealing.

## D. *Ink Continuity and Printing Interconnects on Irregular Surfaces*

Printing on irregular surfaces enables the fabrication of more flexible and wearable electronics. This advancement opens new applications ranging from healthcare to aerospace with significant enhancement in the functionality and performance of electronic devices. Since the particle-free ink printed interconnects are very thin, it was necessary to evaluate their ability to be printed on irregular surfaces. As a test case we connected a silicon die with a surface-deposited interconnect with a dielectric ramp connecting the substrate and the top of the die.

As shown in Fig.6, dielectric (NEA 123) lines were printed using the "NORDSON EFD PRO4" dispenser system. The thickness of the dielectric structure was measured to be 65 µm and the silver traces were printed using the AJP at a direction orthogonal to that of the dielectric print. The resultant film was photonically cured with a flash lamp energy of 3.81 J/cm$^2$. No electrical disconnections occurred in the printed silver films and the resistance of these films ranged from 5.77 Ω to 7 Ω as shown in Fig. 6 (b), demonstrating robust conductivity and post-curing durability.

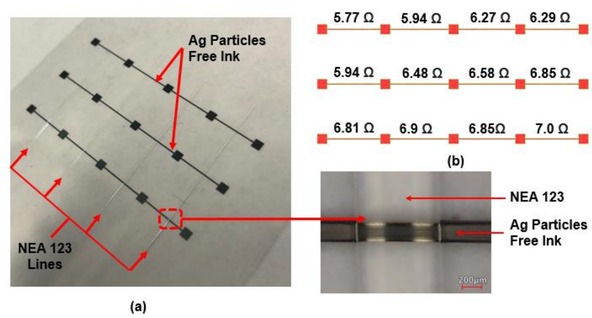


Fig. 6: (a) Printed Ag films on the irregular surface of PET and dielectric lines, (b) Resistance measurements after photonic curing.

Developing microelectronics packaging is necessary to improve printed interconnects between the substrate and die. The interconnects enable the integration of high-performance and small devices. The process of printing particle-free Ag ink interconnects was optimized. First, a suitable surface for the printed interconnects were dispensed around the die to form a smooth transition from the die to the PET substrate; the dielectric NEA123 was UV cured at 200 mW/cm$^2$ for 30 secs. As shown in Fig.7 (a), the interconnects were printed from the Si die into the PET substrate. 200 µm diameter pads (25 nos.) and 300 µm ones (12 nos.) were printed to investigate the footprint area that can be obtained on 3x3 mm Si die. Three layers were printed using AJP and the thickness of the printed traces was measured to be 0.37µm with a resistance ranging between 6-8 Ω.

A daisy chain was printed to link several test pads in a sequential chain as shown in Fig. 7 (b). This prototyping allows for the evaluation of the continuity of printed particle-free ink over non-flat surfaces. The average resistance at different sides of the daisy chain is 32.4 Ω, which demonstrates the stability of printed silver particle-free ink over irregular objects.

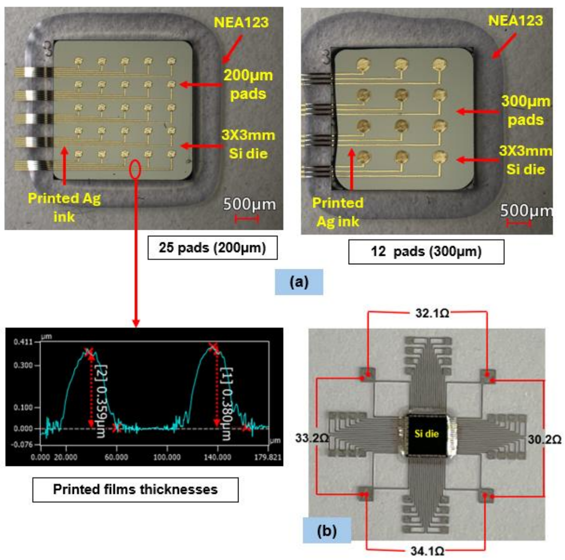


Fig. 7: (a) Printed traces with different number of pads and sizes on Si dies, (b) Printed daisy chain between dog bone pads on Si die and PET substrate.

## *E. Current Carrying Capacity of Particle-free Ag Ink*

The current carrying capacity test was performed using Keithley 2636B system source meter to study the capabilities and the electrical performance of particle-free ink printed traces. It assesses the electrical current that can safely flow across a printed film before failure. The test was performed for the Ag particle-free ink as well as for a more conventionally used nanoflake Ag ink to compare ink performance. The printed test vehicle design, shown in Fig. 8 (a), has dimensions of 11 mm length, 0.225 mm width and 2 mm x1 mm probe pads. The test vehicle was constructed by dispensing a dielectric layer (NEA 123) using the "NORDSON EFD PRO4" system on a copper substrate, then printing the Ag traces using the AJP 3X and curing at 140°C for 1 hour. As shown in Fig.8 (b) & (c), the thickness of both printed Ag inks varied with trace position, although the maximum thickness was around 1.5 µm for the particle-free ink and 4.5 µm for the nanoflake ink. However, the printed samples were normalized per area for both inks using Python code to calculate the current density at the failure point.

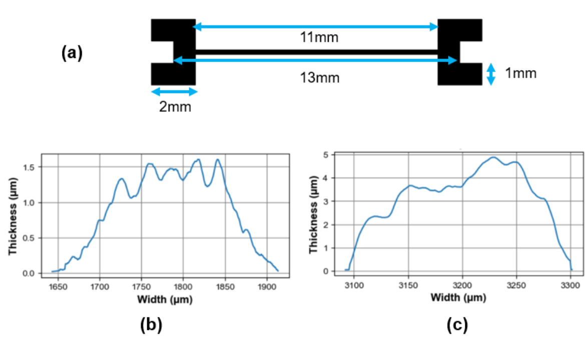


Fig. 8: (a) Test vehicle design, (b) Printed particle-free Ag ink trace profile, (c) Nanoflake based Ag ink printed profile.

A pulsed current was applied, gradually increasing by 5 mA every 10 seconds until conductor failure. The maximum current carrying capacity is the highest electrical current the conductive trace can carry until permanent failure or damage. As shown in Fig.9 (a) and (b), the applied current causes the conductive trace resistivity to increase, which is expected due to the thermal coefficient of resistance (TCR). The resistivity increases as the temperature increases due to increased collision rate between electrons and phonons. Passing an electrical current through a conductor converts the electrical energy into heat energy which is known as "Joule Heating". Beyond a critical current density, the inks demonstrate an inverse correlation of resistance with current. It is believed that Joule heating induces further thermal sintering of the microstructure, driving grain growth and reducing the occurrence of electron scattering at grain boundaries. Finally, the current density will be high enough to damage the printed traces and the substrate. The printed particle-free Ag ink traces failed at $2.022 \times 10^5 \pm 0.2$ A/cm$^2$,

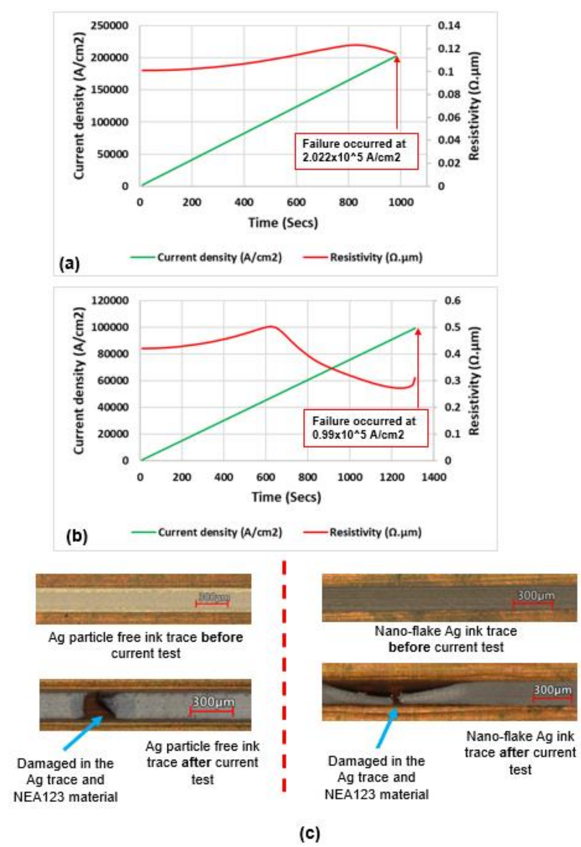


Fig. 9: Resistivity changes over time and current density for (a) Particle-free Ag ink and (b) Nanoflake-based Ag ink. (c) Printed traces before and after current test.

while the traces printed with nanoflake-based Ag ink occurred at $0.99 \times 10^5 \pm 0.18$ A/cm$^2$. The particle-free ink failed at approximately double the value of the nanoflake ink, indicating a greater resilience to electromigration and making it an attractive material for high-power electronic applications. Near failure, the traces of both inks were delaminated and damaged due to the increment in the current that increased the temperature rapidly within the printed trace, leading to a reduced cross-section area of the trace as shown in Fig.9 (c). As the high temperature affects the NEA123 material's thermal stability, the material expanded around the trace, causing it to fail. It is observed that changes occurred in the microstructure of the traces after the current test due to the further sintering of the traces. The nanoflake-based Ag trace became smoother, and bonding occurred between the nanoflake microstructure.

## IV. CONCLUSIONS

Improving materials and additive manufacturing technologies is necessary in the electronics industry. Enhancing the quality, adhesion, and conductivity of printed traces will result in more miniaturized and efficient electronic components. The particle-free ink shows excellent adhesion on PET and NEA123 substrates, while it has poor adhesion on PI and glass substrates. Photonic annealing improves the film's conductivity up to four times the conductivity of thermally annealed films due to the formation of metallic needles in the ink microstructure. This work shows also some of the limitations of the particle-free ink; firstly, good adhesion is highly substrate-dependent. Additionally, the printed thin layers of material make it sensitive to the substrate surface roughness and ambient conditions that can significantly influence the conductivity of the printed features. The particle-free Ag ink shows promising continuity on irregular surfaces with satisfactory conductivity. The failure of the current carrying capacity test of particle-free Ag ink occurred at the double the current density rate compared to the nanoflake ink films, making it attractive in high-power electronics applications. Overall the particle-free Ag ink showed significantly improved properties compared to conventional nanoflake-based inks and makes it an attractive alternative to conventional approaches. In future work, the particle-free Ag ink thermal conductivity will be estimated and validated using frequency domain thermoreflectance (FDTR) test at various curing conditions to provide guidance on electronic device heat management. Moreover, reliability performance assessments of the Ag interconnects will be performed.

## References


[1] Yang, W., List-Kratochvil, E. J., & Wang, C. (2019). Metal particle-free inks for printed flexible electronics. Journal of Materials Chemistry C, 7(48), 15098-15117.doi. 10.1039/C9TC05463D.

[2] Yang, W., Hermerschmidt, F., Mathies, F., & List-Kratochvil, E. J. (2021). Comparing low-temperature thermal and plasma sintering processes of a tailored silver particle-free ink. Journal of Materials Science: Materials in Electronics, 32, 6312-6322. doi.org/10.1007/s10854-021-05347-1

[3] A. S. Obeidat *et al*., "Performance Evaluation of RF Novel Microstrip Lines Printed on Flexible Substrates," *2023 IEEE 73rd Electronic Components and Technology Conference (ECTC)*, Orlando, FL, USA, 2023, pp. 1471-1477, doi: 10.1109/ECTC51909.2023.00250.

[4] R. Al-Haidari *et al*., "Planar SiC Power Module Packaging and Interconnections Using Direct Ink Writing," *2023 IEEE 73rd Electronic Components and Technology Conference (ECTC)*, Orlando, FL, USA, 2023, pp. 668-675, doi: 10.1109/ECTC51909.2023.00117.

[5] N. J. Wilkinson, M. A. A. Smith, R. W. Kay, and R. A. Harris, "A review of aerosol jet printing—a non-traditional hybrid process for micro-manufacturing," International Journal of Advanced Manufacturing Technology, vol. 105, no. 11, pp. 4599–4619, Dec. 2019, doi: 10.1007/s00170-019-03438-2.

[6] Jignasu, A., Rurup, J. D., Secor, E. B., & Krishnamurthy, A. (2024). NURBS-based path planning for aerosol jet printing of conformal electronics. Journal of Manufacturing Processes, 118, 187-194. doi.org/10.1016/j.jmapro.2024.03.031.

[7] A. S. Obeidat *et al*., "Effect of Thermal and Mechanical Stresses on Novel Microstrip Lines Printed on Flexible Substrates," in *IEEE Transactions on Components, Packaging and Manufacturing Technology*, vol. 14, no. 8, pp. 1481-1492, Aug. 2024, doi: 10.1109/TCPMT.2024.3412740.

[8] Grant, T. D., Hourd, A. C., Zolotovskaya, S., Lowe, J. B., Rothwell, R. J., Jones, T. D., & Abdolvand, A. (2022). Inkjet printing of high-concentration particle-free platinum inks. Materials & Design, 214, 110377. doi.org/10.1016/j.matdes.2021.110377.

[9] Hu, M., Cai, X., Guo, Q., Bian, B., Zhang, T., & Yang, J. (2016). Direct pen writing of adhesive particle-free ultrahigh silver salt-loaded composite ink for stretchable circuits. ACS nano, 10(1), 396-404. doi.org/10.1021/acsnano.5b05082.

[10] Hu, M., Cai, X., Guo, Q., Bian, B., Zhang, T., & Yang, J. (2016). Direct pen writing of adhesive particle-free ultrahigh silver salt-loaded composite ink for stretchable circuits. ACS nano, 10(1), 396-404. doi.org/10.1021/acsnano.5b05082.

[11] Smith, M., Choi, Y. S., Boughey, C., & Kar-Narayan, S. (2017). Controlling and assessing the quality of aerosol jet printed features for large area and flexible electronics. Flexible and Printed Electronics, 2(1), 015004.doi. 10.1088/2058-8585/aa5af9.

[12] Lall, P., Goyal, K., Leever, B., & Miller, S. (2019, May). Factors influencing the line consistency of commonly used geometries for additively printed electronics. In 2019 18th IEEE Intersociety Conference on Thermal and Thermomechanical Phenomena in Electronic Systems (ITherm) (pp. 863-869). IEEE. doi: 10.1109/ITHERM.2019.8757308.

[13] Park, S., Vosguerichian, M., & Bao, Z. (2013). A review of fabrication and applications of carbon nanotube film-based flexible electronics. Nanoscale, 5(5), 1727-1752. doi. 10.1039/C3NR33560G.

[14] Wilkinson, N. J., et al. "A Review of Aerosol Jet Printing—a Non-Traditional Hybrid Process for Micro-Manufacturing." The International Journal of Advanced Manufacturing Technology, vol. 105, no. 11, 2019, pp. 4599–619. Crossref, https://doi.org/10.1007/s00170-019-03438-2.

[15] Smith, Michael, et al. "Controlling and Assessing the Quality of Aerosol Jet Printed Features for Large Area and Flexible Electronics." Flexible and Printed Electronics, vol. 2, no. 1, 2017, p. 015004. Crossref, https://doi.org/10.1088/2058-8585/aa5af9.

[16] H. Kim, J. S. Horwitz, G. P. Kushto, Z. H. Kafafi, and D. B. Chrisey, "Indium tin oxide thin films grown on flexible plastic substrates by pulsed-laser deposition for organic light-emitting diodes," Appl Phys Lett, vol. 79, no. 3, pp. 284–286, Jul. 2001, doi: 10.1063/1.1383568.

[17] A. S. Obeidat *et al*., "Embedded RF Packaging Via Ceramic 3D Printing and Printed Electronics Additive Manufacturing," *2024 IEEE 74th Electronic Components and Technology Conference (ECTC)*, Denver, CO, USA, 2024, pp. 685-692, doi: 10.1109/ECTC51529.2024.00112.

[18] S. Lieberman et al., "Electrical Behavior of Thin Die Assembly on Flexible Substrate Under Vibration Testing," 2024 IEEE 74th Electronic Components and Technology Conference (ECTC), Denver, CO, USA, 2024, pp. 1670-1676, doi: 10.1109/ECTC51529.2024.00276.